As–cast microstructures of HEA designed to be strengthened by HfC

PATRICE BERTHOD[*]

Faculté des Sciences et Technologies, Université de Lorraine, Campus Victor Grignard, 54500 Vandoeuvre–lès–Nancy, France
Institut Jean Lamour, Université de Lorraine, Campus Artem, 2 allée André Guinier, 54000 Nancy, France

Abstract. In this study, two new alloys, resulting of the addition of carbon and hafnium to a well–known high entropy alloy (HEA) – the equimolar CoNiFeMnCr one – to promote the formation of HfC carbides, were produced by conventional casting under inert atmosphere and characterized. The as–cast microstructures of the obtained HEA/HfC alloys were studied by X–ray diffraction, electron microscopy, energy dispersion spectrometry, and Vickers indentation. These HEA/HfC alloys are double–phased, with an austenitic matrix and interdendritic eutectic script–like HfC carbides. In terms of chemical composition and of crystallographic network, the matrix of the alloys is identical to the CoNiFeMnCr alloy. In that way, the two alloys can be considered as composite materials resulting of a HEA matrix strengthened by hard HfC particles.

Keywords: HEA alloys, HfC carbides, Microstructure, XRD, Electron microscopy, Hardness.

Introduction

The "high entropy alloy" principle (HEA), which has appeared during the past decade, is at the origin of one of the new families of high temperature alloys presenting high potential for many applications such as aeronautics (turbine disks and blades), power generation (burners, hottest parts of turbines) and industrial processes (tools for shaping molten glasses), for instance. Notably, they may possibly replace superalloys [1–3] due to their high temperature mechanical properties and to the decrease in content of "critical elements" (Co and Ni for instance) in their chemical compositions. HEAs contain, in equimolar quantities, various metals, and some of them belong to the {Co, Ni, Fe, Cr, Mn} system [4, 5].

---

[*]Correspondence address: patrice.berthod@univ-lorraine.fr

The thermodynamic description of this quinary system was studied until recently [6, 7]. Equimolar FeCoNiCrMn alloys are often elaborated by conventional foundry but other ways of elaboration of superalloys can be considered for obtaining these HEAs: single crystalline solidification [8], three–dimensions printing [9] or thin film formation [10]. Recent works have explored their behaviors when solicited extreme conditions: mechanical resistance [11, 12] or resistance against chemical aggressions at high temperature [13]. The evolutions of microstructures and properties in case of the variation of the Co or Ni contents [14] in their chemical compositions (and even the suppression of Co [15] or of Ni [16]) were also recently subjected to investigations. Some HEA even became "Medium Entropy Alloys" [17]. Nanoparticles of SiC particles have also started to be added in HEAs [18].

The equimolar FeCoNiCrMn alloys are far from classical superalloys hardened by solid solution, based on cobalt for instance. It is not very different from the matrix of polycrystalline cobalt superalloys with interdendritic spaces reinforced by carbides. Effectively, the superalloys based on cobalt generally also contain nickel and chromium, with contents possibly equal to several tens weight percent. The weight contents are not really the same (in the cobalt alloys: 50 wt.%Co or a little more, 10 wt.%Ni and 30 wt.%Cr), but it is possible to think that HEAs containing these elements are able to also contain primary chromium carbides or MC carbides as additional phases, useful to achieve better mechanical properties for high temperature service. Notably, significant hardening can be expected from the use of HfC carbides, which were recently successfully tested in polycrystalline chromia–forming cobalt–based model alloys [19, 20].

The purpose of this study is to investigate the as–cast microstructures and room temperature hardness of new superalloys resulting of the association of a HEA dendritic matrix and of an interdendritic network made of script–like MC carbides. It focuses on two HEA–based alloys in which the appearance of HfC carbides is favored by the introduction of carbon and of hafnium in adequate quantities [19, 20].

Methodology

Thus, two novel alloys were considered in this study. Both are extrapolated from a HEA alloy chosen among the most classical ones: the equimolar CoNiFeCrMn alloy [4, 5]. The two alloys produced and studied here result from this HEA to which two amounts of carbon and two amounts of hafnium were added. These two {Hf, C}–containing HEA alloys are a 96(CoNiFeCrMn)–0.25C–3.72Hf alloy (from now called "HEA/HfC1") and a 92(CoNiFeCrMn)–0.50C–7.44Hf alloy (from now called "HEA/HfC2"), with all contents being expressed in weight percent. In both cases a total charge of about 40g composed of pure elements (purity > 99.9 wt.%, Alfa Aesar and Aldrich) was prepared.

Each charge was placed in the copper crucible of a high frequency induction furnace (CELES, France; maximal power: 50kW). This metallic crucible was

permanently cooled by a continuous flow of water at ambient temperature during all elaboration steps.

Once the mix of pure elements was deposited in the crucible, a silica tube was placed to allow the evacuation of the present air from the fusion chamber and to replace it by pure argon (final pressure: several hundreds of millibars). The water–cooled copper coil surrounding tube and crucible allowed generating an alternative magnetic field (level of frequency: 100 kHz, applied voltage up to 5kV).

The melting of the mix of pure elements and the isothermal chemical homogenization of the obtained liquid alloy were achieved after less than five minutes, and during fifteen minutes, respectively. The cooling was operated by decreasing the input power/voltage. First the alloy solidified, and later it cooled in solid state. After about 20 to 30 minutes, the temperature of the obtained ingots was low enough to be extracted from the crucible and handled for further manipulations.

Each ingot was embedded in a cold resin mixture (ESCIL, France) to allow cutting being easier. Cutting was carried out using a metallographic saw, and samples with the adequate shapes and sizes to prepare metallographic samples were obtained. The cut part was itself embedded in the cold resin mixture and the resulting metallographic samples were ground then finished with SiC paper starting at the #600-grade SiC papers and ending with a textile disk enriched with 1 µm hard particles.

Each mirror–like sample was subjected to X–ray diffraction, using a D8 Advance diffractometer from Bruker (wavelength of the K_α transition of Cu). It was also placed in the chamber of a Scanning Electron Microscope (JSM-6010LA from JEOL, Japan) to observe its microstructure in Back Scattered Electrons mode under 15kV (acceleration voltage). The obtained chemical composition was controlled by Energy Dispersive Spectrometry (full frame analysis at the ×250 magnification). EDS spot analyses were carried out on the coarsest particles to identify them and to specify the chemical composition of the matrix.

In addition, the alloys were also subjected to indentation tests to evaluate their hardness. This was done using a Presi (France) automatic indentation machine (Vickers penetrator, load: 10kg, five indentations per alloy).

Results and discussion

Global microstructures and compositions

The X–ray diffractograms obtained for the microstructures of the two alloys resulting from the addition of hafnium and carbon are presented in Figure 1 (HEA/HfC1) and in Figure 2 (HEA/HfC2). In both diffractograms all the peaks corresponding to the Face Centered Cubic CoNiFeMnCr solid solution are present. The other peaks correspond to the HfC phase. The microstructures of these two {Hf, C}–containing alloys are illustrated by SEM/BSE micrographs in Figure 3

(HEA/HfC1) and in Figure 4 (HEA/HfC2), together with the EDS spectra acquired on these zones (full frame analysis).

According to the diffractograms (Figure 1, Figure 2), both alloys contain only two phases: a dendritic matrix and HfC carbides. No other peaks are present. The HfC peaks obtained for the HEA/HfC2 alloy being higher than the ones obtained for the HEA/HfC1 alloy, one can expect the presence of more HfC carbides in the HEA/HfC2 alloy than in the other alloy.
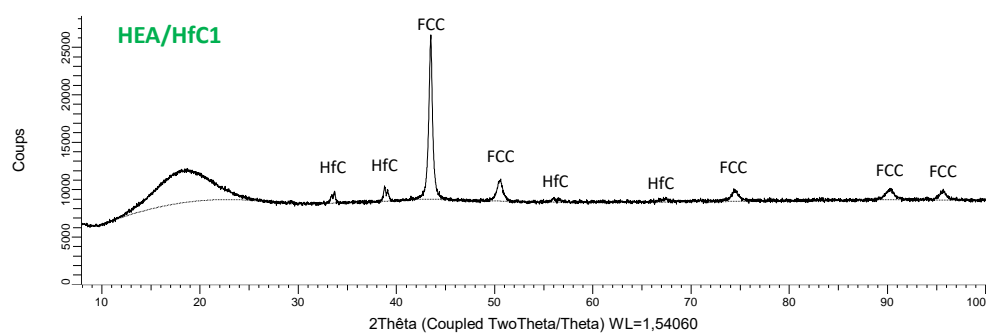

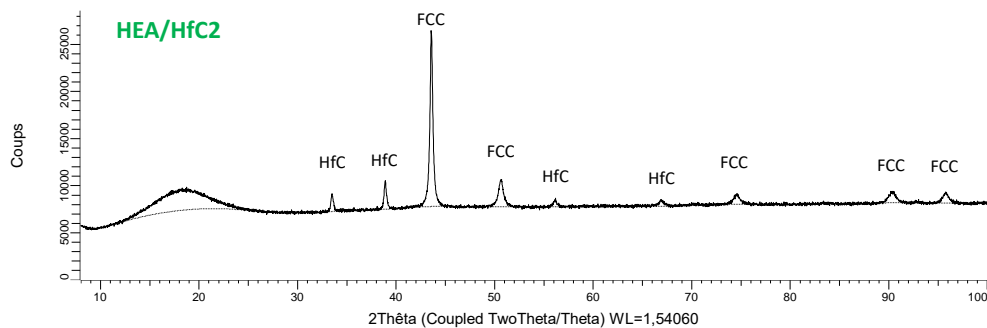Fig. 1. Diffractogram corresponding to the HEA/HfC1 alloy.

Fig. 2. Diffractogram corresponding to the HEA/HfC2 alloy.

This is exactly what one can observe in the microstructures (Figure 3, Figure 4). First, both alloys are made of a dendritic matrix and of hafnium monocarbides (HfC are all the particles appearing white in BSE mode), with more HfC in the HEA/HfC2 alloy than in the other alloy. This difference appears as logical, taking into account the differences in carbon contents between the two alloys. In fact, in both cases, the HfC carbides are present with two distinct forms: script–like white carbides homogeneously distributed in the whole microstructure, and as clusters of blocky white carbides present here and there. The EDS spot analyses performed on the coarsest white particles of each of the two types allowed confirming that the

stoichiometry is HfC in both cases. This particular type of microstructure with these two different geometries of the HfC carbides is the same as the ones earlier encountered in cobalt–chromium alloys [21].
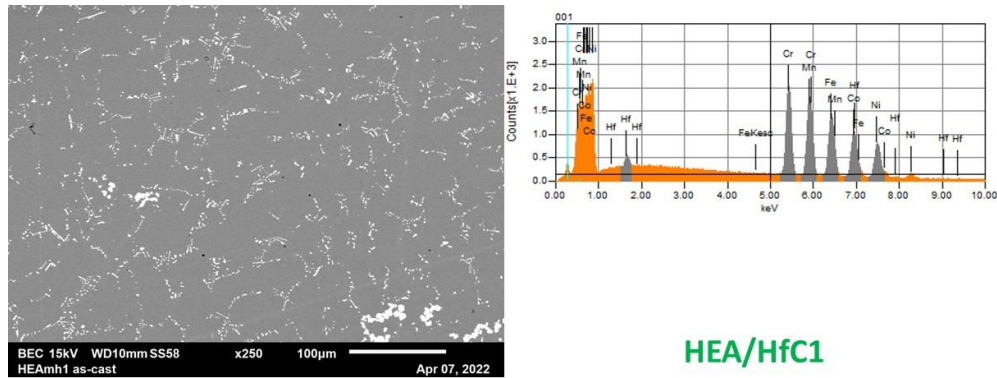

Fig. 3. SEM/BSE micrograph of the microstructure of the HEA/HfC1 alloy (left) and EDS spectrum acquired on this area (right).
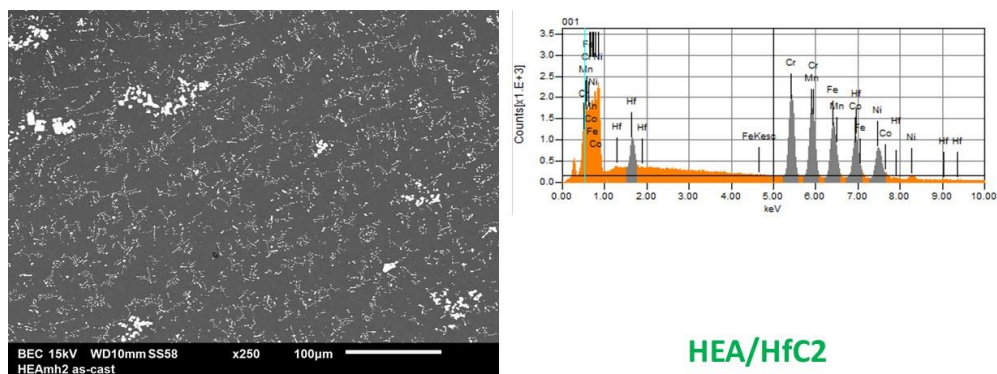

Fig. 4. SEM/BSE micrograph of the microstructure of the HEA/HfC2 alloy (left) and EDS spectrum acquired on this area (right).

The global chemical compositions of these two alloys were measured by full frame EDS analysis on three randomly chosen zones (magnification ×250). Results are displayed in Table 1 (HEA/HfC1) and in Table 2 (HEA/HfC2). They demonstrate that the compositions initially wished for the alloys are well respected.

Table 1. General chemical composition of the HEA/HfC1 alloy (average and standard deviation calculated from the results of three ×250 full frame areas); all contents in weight percent, carbon not possible to analyze but supposed to be well respected: 0.25 wt.%C)

HEA/HfC1 Whole alloy	Wt.% Co	Wt.% Ni	Wt.% Fe	Wt.% Mn	Wt.% Cr	Wt.%Hf
Average content	19.9	20.2	18.4	18.2	19.3	4
Standard deviation	0.3	0.6	0.4	0.2	0.5	1.9

Table 2. General chemical composition of the HEA/HfC2 alloy (average and standard deviation calculated from the results of three ×250 full frame areas); all contents in weight percent, carbon not possible to analyze but supposed to be well respected: 0.5 wt.%C)

HEA/HfC2 Whole alloy	Wt.% Co	Wt.% Ni	Wt.% Fe	Wt.% Mn	Wt.% Cr	Wt.%Hf
Average content	19.0	19.9	18.1	17.0	19.1	7.0
Standard deviation	0.4	0.5	0.3	0.3	0.2	0.8

Characteristics of matrix and of carbides

The matrix is obviously single–phased, with only an austenitic crystalline structure. Its chemical composition was assessed by spot analysis in three different locations. This led to the matrix compositions presented in Table 3 (HEA/HfC1) and in Table 4 (HEA/HfC2). Three remarkable observations are to be done about the results. First, the Co, Ni, Fe, Mn and Cr contents are the same as in the whole alloy. Second, the results concerning Fe and Mn are rather scattered, with high values of the standard deviation and values of average content higher or lower than the Fe and Mn contents in the whole alloy. Third, hafnium can be considered as totally absent in the matrix. The distribution of all elements in the microstructures is illustrated by the elemental X–map acquired in the HEA/HfC2 alloy microstructure using the EDS device equipping the SEM. The element images clearly show that the matrix is rather homogeneous in Co, Ni and Cr, and contains Fe and Mn in a heterogenous manner: Mn is more present in the interdendritic spaces than in the cores of the dendrites while this is the inverse disposition for Fe. Obviously, Mn was rejected in the liquid during the dendrite growth while Fe was concerned by negative segregation. It is also to point out that Hf is effectively totally absent in the matrix, which is consistent with the EDS spot analysis results. Hf and C are clearly concentrated in the white particles.

Table 3. Chemical composition of the matrix of the HEA/HfC1 alloy
(all contents in weight percent, carbon not analyzed)

HEA/HfC1 Matrix	Wt.% Co	Wt.% Ni	Wt.% Fe	Wt.% Mn	Wt.% Cr	Wt.%Hf
Average content	21.1	19.7	21.6	16.8	20.7	0.1
Standard deviation	1.2	0.7	1.6	1.8	0.3	0.1

Table 4. Chemical composition of the matrix of the HEA/HfC2 alloy
(all contents in weight percent, carbon not analyzed)

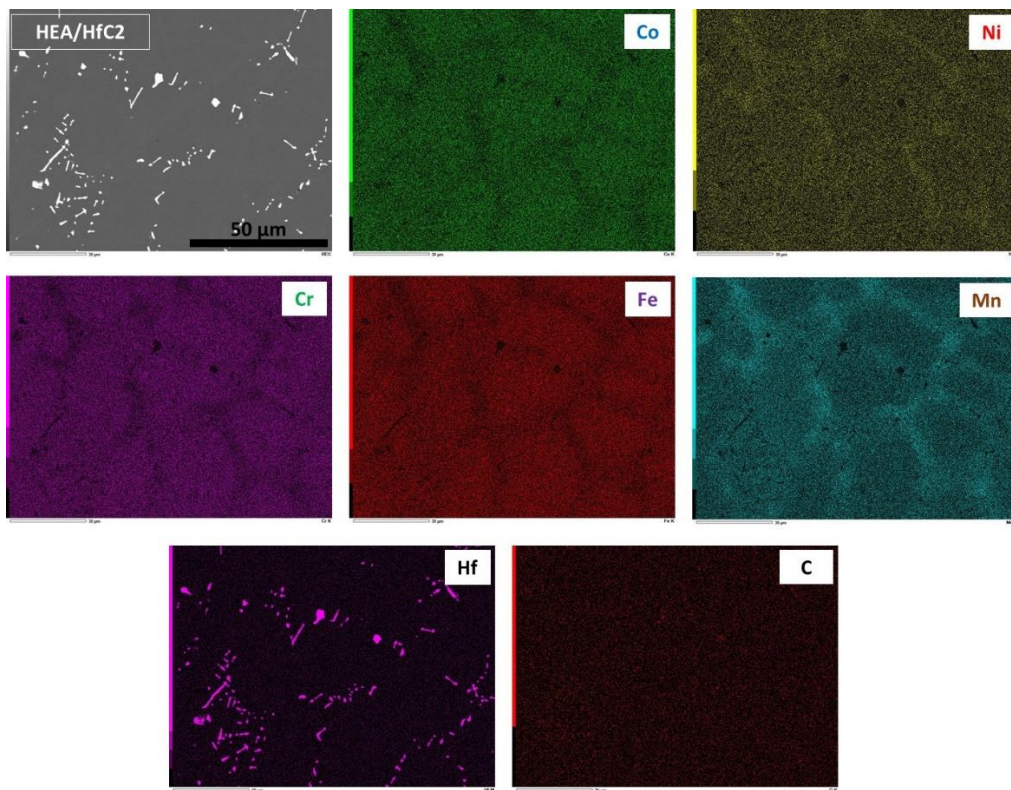| HEA/HfC2 Matrix	Wt.% Co	Wt.% Ni	Wt.% Fe	Wt.% Mn	Wt.% Cr	Wt.%Hf
Average content	18.9	23.2	16.6	22.7	18.6	0.0
Standard deviation	2.7	3.6	4.4	6.0	2.5	0.0

Fig. 5. Elemental EDS X–map acquired in the microstructure of the HEA/HfC2 alloy.

The blocky particles (gathered in isolated clusters) and the script–like particles, all identified above as HfC carbides thanks to XRD and spot EDS analysis, constitute the second phase. The blocky HfC are coarser than the script–like ones, and they can be clearly examined in Figure 3 and Figure 4. These curious particles, similar to the pre–eutectic HfC earlier observed cobalt–chromium alloys rich in C and Hf [21], were probably the first solid to appear at the start of solidification, as previously concluded in the cobalt–chromium alloys cited above [21]. The script–like HfC, which are the most present in both alloys, are finer. Detailed observation of their morphology is possible in the high magnification SEM/BSE micrographs presented in Figure 6. In contrast with the clusters of pre–eutectic blocky HfC which seem independent on the matrix, these script–like HfC are systematically located in the interdendritic spaces where they are closely mixed with matrix. Their specific locations and imbrication with matrix appears as very favorable to a strong cohesion between neighboring dendrites and between neighboring grains. One can thus expect an efficient resistance to the tertiary stage of creep at high temperature.

Hardness results

Per alloy, five indentations were carried out according to the Vickers method, with a 10kg load. The results, displayed in Table 5, are available for comparison with the hardness of a HEA reference alloy recently studied [22] (the cast equimolar CoNiFeMnCr alloy). It appears clearly that the presence of the HfC carbides induced a significant increase in hardness. The obtained level of hardness is an additional indication expecting good creep resistance at elevated temperature but it is not high enough to cause difficulties of machining.
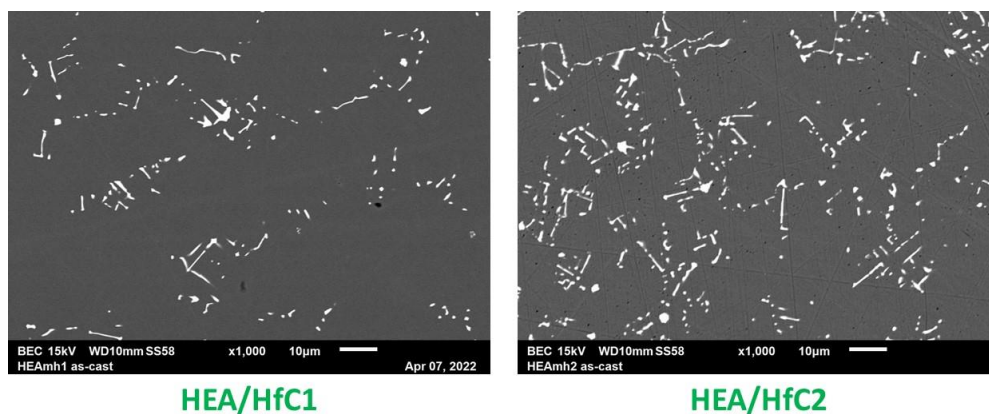

HEA/HfC1   **HEA/HfC2**

Fig. 6. High magnification SEM/BSE micrographs for observation in details of the microstructures (left: HEA/HfC1, right: HEA/HfC2).

Table 5. Hardness of the HEA/HfC alloys
in comparison with the HEA reference alloy [22]

Vickers 10 kg 5 indent.	HEA ref.	HEA/HfC1	HEA/HfC2
Average content	121	157	162
Standard deviation	2	12	5

Conclusion

HEA alloys in general, and HEAs of the equimolar CoFeNiMnCr type in particular, are currently promising alloys, as they are and also as bases for more complex alloys, for many applications requiring notably high mechanical properties. Some of them can be successfully elaborated by classical foundry, and, in this study, the two alloys conventionally cast with addition of Hf and C just demonstrate that microstructures looking like high performance polycrystalline cobalt–chromium superalloys strengthened by script–like eutectic interdendritic hafnium monocarbides can be obtained, with only one difference: the matrix is not a Hf–free cobalt–chromium matrix, but a Hf–free equimolar CoNiFeMnCr matrix. It is true that, in the as–cast state after a rather fast cooling this one is not yet chemically homogeneous (Mn segregation during solidification) but this can be easily corrected by a short homogenization heat treatment at high temperature, without any destabilization of the HfC carbides which are recognized for their high stability in volume fraction and morphology. Outlooks concerning this new type of composite materials – {HEA matrix, HfC reinforcing particles} – are further investigations concerning their high temperature properties (behaviors in high temperature oxidation and corrosion, creep resistance…), to explore and check the high performance promised by this association of two phases, CoFeNiMnCr FCC solid solution and script–like interdendritic HfC. This is currently the subject of an ongoing work.

Acknowledgments

References

[1]   Sims C.T., Hagel W.C., *The Superalloys-Vital High Temperature Gas Turbine Materials for Aerospace and Industrial Power*, John Wiley & Sons, 1972.
[2]   Sims C.T., Stoloff N.S., Hagel W.C., *Superalloys II. High Temperature Materials for Aerospace and Industrial Power*, John Wiley & Sons, 1987.

[3]   Kracke A., *Superalloys, the most successful alloy system of modern times – Past, Present and Future*, in Proceedings of the 7th International Symposium on Superalloy 718 and Derivatives (Edited by: E. A. Ott, J. R. Groth, A. Banik, I. Dempster, T. P. Gabb, R. Helmink, X. Liu, A. Mitchell, G. P. Sjöberg and A. Wusatowska-Sarneck), TMS (The Minerals, Metals & Materials Society), 2010.

[4]   Liu S.F., Wu Y., Wang H.T., He J.Y., Liu. J.B., Chen C.X., Liu X.J., Wang H., Lu Z.P., *Intermetallics*, **93**, p. 269–273.

[5]   Ferrari A., Körmann F., *Applied Surface Science*, **533**, 147471, 2020.

[6]   Wilson P., Field R., Kaufman M., *Intermetallics*, **75**, p. 15–24, 2016.

[7]   Do H.S., Choi W.M., Lee B.J., *Metals and Corrosion*, **57**, p. 1373–1389, 2022.

[8]   Kawamura M., Asakura M., Okamoto N. L., Kishida K., Inui H., George E.P, *Acta Materialia*, **203**, 116454, 2021.

[9]   Osintsev K., Konovalov S., Zaguliaev D., Ivanov Y., Gromov V., Panchenko I., *Metals*, **12**, 197, 2022.

[10]   Hu M., Cao Q.P., Wang X.D., Zhang D.X., Jiang J.Z., *Metals*, **12**, 197, 2022.

[11]   Mehranpour M. S., Shahmir H., Nili-ahmadabadi M., *Materials Letters*, **288**, 129359, 2021.

[12]   Xiao H., Zeng Q., Xia L., Fu Z., Zhu S., *Materials and Corrosion*, **73**, p. 550–557, 2022.

[13]   Kim Y.K., Joo Y.A., Kim H.S., Lee K.A., *Intermetallics*, **98**, p. 45–53, 2018.

[14]   Zhu Z.G., Ma K.H., Yang X., Shek C.H., *Journal of Alloys and Compounds*, **695**, p. 2945–2950, 2017.

[15]   Dong J., Feng X., Hao X., Kuang W., *Scripta Materialia*, **204**, 114127, 2021.

[16]   Zhang C., Zhang F., Jin K., Bei H., Chen S., Cao W., Zhu J., Lv D., *Journal of Phase Equilibria and Diffusion*, **38**, p. 434–444, 2017.

[17]   Bracq G., Laurent-Brocq M., Varvenne C., Perrière L., Curtin W.A., Joubert J. M., Guillot I., *Acta Materialia*, **177**, p. 266–279, 2019.

[18]   Szklarza Z., Lekki J., Bobrowski P., Szklarza M. B., Rogal Ł., *Materials Chemistry and Physics*, **215**, p. 385–392, 2018.

[19]   Berthod P., Conrath E., *Journal of Materials Science and Technology Research*, **1**, p. 7–14, 2014.

[20]   Conrath E., Berthod P., *Materials Science,* **53**, p. 861–867, 2018.

[21]   Berthod P., Conrath E., *Materials Chemistry and Physics,* **143**, p. 1139–1148, 2014.

[22]   Berthod P., *Journal of Metallic Material Research*, submitted.